Gaz dans les Solutions Aqueuses," Chim. Ind. XXI^{me} Congr. Int. Chim. Ind., Soc. Chim. Ind., Paris, p. 168 (1948).
Vinograd, J. R., and J. W. McBain, "Diffusion of Electrolytes and of the Ions in Their Mixtures," *J. Am. Chem. Soc.*, 63, 2008 (1941).

APPENDIX A: THE PHYSICAL SOLUBILITY OF SULFUR DIOXIDE IN AQUEOUS SODIUM BISULFITE SOLUTIONS

The physical solubility of a gas in aqueous electrolyte solutions can be correlated by the following expression (van Krevelen and Hoftijzer, 1948):

$$\log(A_i/A_{iw}) = -k_s I \qquad (17)$$

The coefficient k_s is the salting-out parameter and is expressed as the sum of the contributions due to the positive and negative ions present and the dissolved gas:

$$k_s = i_+ + i_- + i_g \qquad (A1)$$

The values of i for various ions and gases were reported by van Krevelen and Hoftijzer (1948). However, since the value of i_- for HSO_3^- ions is not known, the salting-out parameter for the sulfur dioxide-sodium bisulfite system cannot be predicted. In the present work, therefore, measurements were made of the total solubility of sulfur dioxide in aqueous sodium bisulfite solutions, from which the physical solubility A_i of sulfur dioxide was calculated by correcting for the effect of the hydrolysis reaction by use of the values for the hydrolysis equilibrium constant reported by Campbell and Maass (1930). The correction was less than 2.8% in the range of the sodium bisulfite concentration covered in the present work.

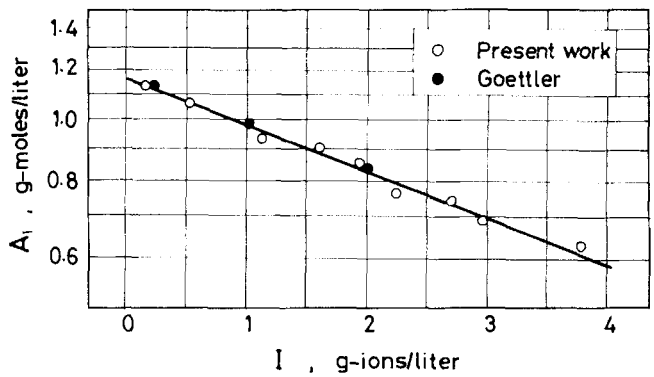

Fig. A-1. Physical solubility of sulfur dioxide into aqueous sodium bisulfite solutions at 25°C.

The results obtained are shown in Figure A1, as a semi-logarithmic plot of A_i against the ionic strength I of the solution. This figure indicates that the physical solubility of sulfur dioxide in aqueous sodium bisulfite solutions is well correlated by Equation (17). In Figure A1, the physical solubility data of Goettler (1967) are also shown. The agreement between the present and Goettler's data is very good. The value of k_s was calculated from the slope of the straight line in Figure A1 as 0.074 l/g-ion. From this value of k_s and the known values of i for sulfur dioxide and Na^+ ions (van Krevelen and Hoftijzer, 1948), the value of i_- for HSO_3^- ions was calculated as 0.085 l/g-ion.

Manuscript received January 3, and accepted March 22, 1977.

Mechanisms and Idealized Dissolution Modes for High Density ($\rho > 1$), Immiscible Chemicals Spilled in Flowing Aqueous Environments

A plausible spill mechanism is proposed and idealized dissolution modes are developed for the prediction of lifetime and downstream cup-mixing concentration of spilled liquids. Four models are developed which reveal that detailed knowledge of the quantity and distribution of geometric shapes that make up the bottom residing interface between the spillage and the overlaying water are the independent variables of primary importance.

L. J. THIBODEAUX

Department of Chemical Engineering
University of Arkansas
Fayetteville, Arkansas 72701

SCOPE

Predictions of the environmental effects of man-made chemicals is increasingly being recognized as a responsibility of the manufacturer of the chemical. A significant number of hazardous chemicals transported upon water routes are more dense than water and come to rest upon the bottom following accidents. Dissolution commences immediately, and the rate determines the in-stream cup-mixing concentration of the spilled chemical. In the interest of protecting stream biota and downstream water users from excessive exposure, a means of predicting chemical concentrations and exposure times likely to result from an inadvertent spill is needed.

Spill mechanisms have been verified in our laboratory. These observations along with previous developments in chemical engineering science have been focused upon a partial solution of this complex problem. Information available on liquid droplet formation from nozzles and coalescence in liquid-liquid extraction provides a fundamental understanding of the mechanism that will produce a bottom residing interface (Meister and Scheele, 1969,

1969*a*; Edge and Kalafatoglu, 1974; Hu and Kintner, 1955; Dzubur and Sawistowski, 1974; Hayworth and Treybal, 1950; Siemer and Kaufman, 1957; Vijayan and Ponter, 1974). Oil spreading on land and water is germane to the liquid chemical spreading on a stream bottom (Fay, 1971; Langmuir, 1933; O'Brien, 1970; Chen et al., 1971). Experimental studies on aqueous dissolution of benzoic acid (Kramers and Kreyger, 1956), hydrocarbon evaporation (Mackay and Matsugu, 1973), and water evaporation (Harbeck, 1962; Schooley, 1969) in simulated and/or actual natural turbulent environment contexts provide a means of estimating interphase mass transfer rates.

This body of knowledge is drawn together and aspects are focused upon the problem of spills involving dense liquid chemicals. A spill mechanism is proposed which explains the creation of a bottom residing chemical-water interface. Idealized geometric forms are invoked as models to represent the dissolution surface area behavior at the chemical-water interface. Realistic predictive techniques are developed for this important class of spilled chemicals.

CONCLUSIONS AND SIGNIFICANCE

The loss of dense liquid chemicals from punctured or otherwise damaged ships and barges or containers aboard such vessels into water is imminent. The spill is completed in a short period of time, typically minutes or hours. A jet of liquid emerges from the rupture but breaks up into globs and droplets. A swarm of small stable drops is formed in deep water. Coalescence occurs as drops arrive at and crowd together upon the stream bottom. For rivers in a nonscouring flow regime, the final resting place of the liquid is dependent upon the morphology of the bottom.

Bottom depressions directly below and downstream of the spill site will contain the spilled liquid. However, some quantity will remain perched upon the relatively flat surfaces above the depressions. Four shapes including constant interface pools, variable interface pools, globs and droplets are invoked to quantify the dissolution interfacial area. In general, the distribution of the mass of spillage into the four shapes is unknown. Equations (18), (20), (22), and (24) give the dissolution time for the various shapes. Equation (27) gives the cup-mixing concentration-time profile of the chemical in the river.

Realistic field experiments of the interfacial area production phenomena and the subsequent dissolution of a dense liquid chemical spilled in a natural flowing setting are costly and possibly polluting in their execution. On-site monitoring of accidental spills does provide field data against which to compare quantitative dissolution models. Documentation on a recent major spill involving chloroform in the Mississippi River provided a test for the dissolution model. A uniform distribution of mass resulted in a predicted maximum water concentration of 809 mg/m^3 chloroform. The maximum field data recorded was 352 mg/m^3. Adjustment of Equation (27) to the concentration-time field data indicates that 73% of the bottom residing liquid was in pools up to one third of a foot (10 cm) in depth. The remaining liquid was inferred to be in the form of globs and drops up to one third of an inch (1 cm) in diameter.

Hazard assessment in the event of spilling a quantity of liquid chemical A in river B is dependent upon a realistic concentration-time prediction. Real world spills involve a complex series of happenings in a complex setting. However, the model developed in this paper provides a plausible qualitative spill description and quantitative expressions to address the problem. This model is significant in that it provides a realistic description for a class of spills which cannot be adequately described by the conventional flow dispersion models.

The accidental spills of materials into rivers, streams, canals, bays, harbors, estuaries, etc., are occurring and will undoubtedly increase as waterborne traffic increases. The spills occur mainly from transportation accidents but can also occur from planned or inadvertent releases from production facilities located near the water body or from routine disposal procedures.

Spills into water can be classified into three main categories (Dahm et al., 1974): soluble compounds in a watercourse, immiscible (slightly soluble or insoluble) compounds that float on water, and immiscible (slightly soluble or insoluble) compounds that sink to the bottom of the watercourse. The first two categories of compounds have received much study, and their behavior is fairly well understood. The last category of compounds has received minimal study and is the topic of this paper.

A recent E.P.A. project report (Pilie et al., 1975) lists 252 recognized hazardous materials having a high probability of being involved in spills into or near watercourses. Of this list, 119, or 47.2%, are "the most difficult-to-treat, hazardous chemicals. . . . which. . . . are heavier than water and highly water soluble."

Spills present a significant threat to public health and welfare. The major modes and amounts of hazardous material transported and forecast for transport in the future have been estimated (Dahm et al., 1974). Water carrier accounts for 23%. Fortunately, there is not necessarily a one-to-one correspondence between quantity manufactured and hazard posed.

The materials most hazardous to the water environment are soluble compounds toxic to the ecosystem at low, critical concentrations. A ranking of chemicals in this group on a combined basis of toxicity and production is available (Dahm et al., 1974). Metal salts also fall into this class of soluble, hazardous materials. The class of hazardous chemicals that are immiscible with water, soluble in water, or slightly soluble with specific gravities greater than unity will sink. These include ethylene dichloride and methyl bromide. Other than detection, notification, and evacuation of the public, little in the way of location, prediction of behavior, and treatment control can be performed on spills involving chemicals in this last category.

Besides describing, in a qualitative fashion, the transformation processes the chemical undergoes during a spill, this paper will provide analytical models for some critical numerical calculations of a predictive nature. These estimates include the downstream mixing cup concentration and spillage residence time on the stream bottom. These two estimates are necessary for decisions associated with water quality, public safety, and ecosystem safety. Average concentration estimates are important with respect to water

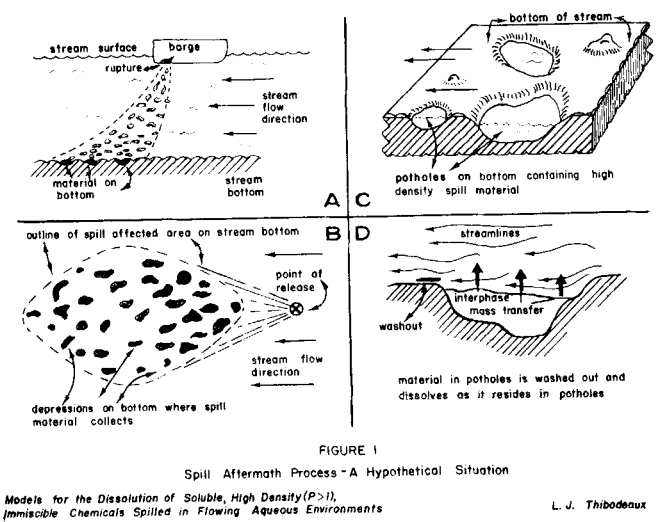

Fig. 1. Spill aftermath process—a hypothetical situation.

quality as reflected in uses as drinking water, industrial water intake, ecosystem exposure, etc. The time of residence of the spillage is important. Knowledge of the rate of mass transfer and the quantity of spillage will allow an estimate of the lifetime of the spillage and the duration of water contamination from it. This time is also important with respect to plans for recovery, cleanup, ecosystem (that is, biota) exposure, alternate water sources for industry and the public, hazard duration, etc.

GENERATION MECHANISM OF SPILLAGE INTERFACE

The natural processes which occur immediately after the spill of a soluble (or slightly soluble), high density, immiscible solid or liquid substance can be anticipated on a gross scale. Figure 1 depicts the processes for a hypothetical spill in a river or similar flowing environment. A barge containing the material in question (for example, chloroform) is involved in an accident which results in the release of a quantity M of the material.

At present, the following sequence of events seems to describe the spill mechanism. Assume that a fairly large hole (> 10 cm) was formed in a river barge type of carrier (see Figure 1) and that a dense liquid is spilled in a deep, slow moving body of water.

1. A jet of liquid emerges from the hole. The jet diameter is the hole diameter.

2. Large globules of liquid emerge from the jet breakup. These globules are roughly the size of the hole.

3. Globules continue to fall through the water. Large globules, settling in water, are unstable and start to break up after falling a short distance.

4. Breakup of droplets and globules continues until a cloud of small, stable droplets (that is, swarm) is formed.

5. Small droplets continue to fall until they make contact with the bottom.

6. As the droplets arrive on the bottom, they tend to accumulate at a specific location downstream from the point of release.

7. As accumulation increases, coalescence commences. Droplets positioned side by side on the bottom coalesce as crowding increases.

8. A continuous film, formed by numerous droplets, may blanket the bottom. Late arriving droplets coalesce at the interface, increasing the film thickness.

9. The size (that is, lateral extent) of the continuous bottom film increases owing to gravity and the drag forces exerted by the flowing water. Spreading occurs by a similar mechanism as oil on open water.

10. A maximum pool size is finally realized.

11. The dissolution process commences.

The above sequence of events has been verified in our laboratory. Small scale spills of bromoform, chloroform, and furfural were observed in both a quiescent drop tank and in a recirculating flume stream simulator. The bottom material in both devices was ungraded silica sand. The quiescent spills were performed upon a leveled sand surface, while a natural surface was used in the stream simulator (Jones and Verser, 1974).

There can and will be many variations on this idealized spill mechanism. If a spill occurs in shallow water, a droplet cloud may never form. The liquid would ooze down in large globule form and cover the bottom. The spill of a small quantity of liquid in deep water may result in the bottom being spattered with individual droplets rather than a continuous film. The droplet cloud consists of a size range of particles. Small droplets move far downstream before they contact the bottom, while large ones contact the bottom nearer the release point.

Stream turbulence in a fast moving body of water can produce significant changes in the above description. Fine droplets remain suspended. A continuous film may never be formed on the bottom. A high liquid velocity keeps the droplets in motion along the bottom. Movement is not unlike the sediment bed load phenomenon that causes sand and silt to move downstream. In this extreme case, the spillage will move out as a slug and behave more or less like the spill of a miscible material.

Most stream bottoms are uneven so that a single pool of uniform thickness is an idealization. Realistically, the dense liquid will accumulate in the lower depression on the bottom. The final resting place scene will be liquid pools of various sizes and shapes scattered over an area downstream from the release point.

Dissolution commences immediately upon water contact and occurs from the globules and droplets in transit to the bottom. Normally, the duration of a spill is short, a few hours at the most, but typically minutes. In the case of slightly soluble materials, the major part of the dissolution will occur while the material resides upon the bottom.

The sequence of events through step *j*, above, describes in an idealized fashion the formation of a zone of contamination on a stream bottom which contains an interface through which mass transfer occurs. This interfacial area between the spillage liquid and the water is an important dependent variable. It seems reasonable to partition the problem analysis into two separate phases. One phase focuses upon a detailed study of the interfacial area and its development from a spill, while the other phase focuses upon the dissolution process and its rate. The forces which create the initial spillage area on the bottom are, for the most part, vastly different from those which affect the dissolution rate once the spillage is in place.

As indicated above, much information exists in the chemical engineering science literature which is directly related to spill mechanisms. The information available on liquid droplet formation and coalescence in liquid-liquid extraction provides a fundamental understanding of the underlying mechanisms that will produce a bottom residing interface (Meister and Scheele, 1969, 1969*a;* Edge and Kalafatoglu, 1974; Hu and Kintner, 1955; Dzubar and Sawistowski, 1974; Hayworth and Treybal, 1950; Siemer and Kaufman, 1957; Vijayan and Ponter, 1974). Oil spreading on land and water is germane to the spreading of SHICHEM* on a stream bottom (Fay, 1971; Langmuir, 1933; O'Brien, 1970; Chen et al., 1971).

* Soluble, *H*igh density, *I*mmiscible *CHEM*icals.

TABLE 1. SUMMARY OF EQUATIONS FOR ESTIMATING MASS TRANSFER COEFFICIENTS

Name/Source	Equation	Limitations	Miss. River chloroform k_x(g-mole/s · m^2)	Equation No.
Laminar flow, flat plate (Bird, *et al.*, 1960)	$k_x = 0.664\, R_e^{-1/2}\, S_c^{-2/3}\, cV_\infty$	$R_e < 10^5$	0.0159	(2)
Turbulent flow, at plates (Treybal, 1968)	$k_x = 0.036\, R_e^{0.8}\, S_c^{1/3}\, c\mathcal{D}_{AB}/L$	$R_e > 10^5$	0.235	(3)
Inclined plane, dissolution benzoic acid (Kramers and Kreyger, 1956)	$k_x = 0.449\, [(g_x\Gamma_v)^{2/3}\, \mathcal{D}_{AB}{}^2/\nu L]^{1/3}\, c$	$R_e \equiv 4\Gamma_v/\nu > 2\,360$	0.266	(4)
Lake surface, water evaporation (Havbeck, 1962)	$k_x = 13.0\, \mathcal{D}_{A,W}{}^{2/3}\, V_8 A_r{}^{-0.5}$	k_x (g · mole/s · m^2), $\mathcal{D}_{A,W}$ (cm^2/s), A_r (ha), V_8 (cm/s), c_m (K_g-mole/m^3), $L(m)$	0.296	(6)
Land spill, hydrocarbon evaporation (Mackay and Matsugu, 1973)	$k_x = 4.96\text{E}4\, L^{-0.11}\, V^{0.78}\, S_c c_m$		0.613	(7)
Wind tunnel, water evaporation (Schooley, 1969)	$k_x = 23.5\, \mathcal{D}_{A,W}{}^{2/3}\, V$		0.868	

DISSOLUTION OF SPILLAGE

The review of the present state of knowledge at this point has been concerned with the processes and mechanisms of the spill phenomenon which influences the production of interface between SHICHEM and the water body. The interface of concern in this analysis is that produced upon the bottom of the water body. This portion of the paper addresses the dissolution process as the SHICHEM resides in place on the bottom. The dissolution which occurs while the SHICHEM is in transit to the bottom may be important, but it is not a primary facet of this work. The transit time in most land bound water bodies (that is, lakes, streams, rivers, reservoirs, etc.) will most probably be short. If a significant amount of dissolution occurs in this short time period, then the spill appears (and behaves for all practical purposes) as the spill of a miscible chemical.

The specific nature of the SHICHEM/water interface is almost completely unknown at this point. At one idealized extreme, the interface may consist of a single large pool of depth h and area A (that is, $A = V/h$). At the other idealized extreme, the interface may be composed of the surface of n droplets of diameter D attached to the bottom (that is, $A = n\pi D^2$). Presumably, a spill onto a bottom containing potholes will create an interface characteristic of the specific bottom conditions (Pilie et al., 1975). Regardless of the specific nature of the actual interfacial area A, there will be a discernible area A_c which will constitute the zone of contamination. Within this area of contamination, the soluble fractions of SHICHEM will be entering the water space.

Interphase mass transfer of component A, at low rates, from the chemical phase to the water phase can be adequately described by the equation

$$W_A = k_X(X_{Ao} - X_{Ab}) \qquad (1)$$

This rate equation assumes that the spilled chemical is a pure material and the resistance to mass transfer is located on the water side. The complexity of the mass transfer process on a stream bottom necessitates the use of the mass transfer coefficient defined in Equation (1). This mass transfer coefficient on the water side must be known to predict the dissolution rate from the zone of contamination. There exist in the literature several equations by which this coefficient can be estimated, and these are summarized in Table 1. These equations reflect both a sound theoretical development and experimental measurements. A brief critical review of the available equations will be given.

Laminar boundary layer theory for tangential flow along a sharp edged, semiinfinite flat plate with mass transfer is well developed. Bird, Stewart, and Lightfoot (1960) summarize this work. For the case of small mass transfer rates, Equation (2) in Table 1 is applicable. The laminar-turbulent transition usually occurs at a length Reynolds number of 10^5. For this theory, the hydrodynamic boundary layer and the diffusional boundary layer commence at the same point (that is, at the sharp edge). For the case of a spilled SHICHEM in a flowing stream, the hydrodynamic boundary layer is developed prior to the flow entering the zone of contamination. A laminar flowing, natural stream is the exception rather than the rule. For these reasons, Equation (2) may not be useful as a realistic estimate of k_x.

Treybal (1968) summarizes mass transfer data for simple situations taken from the literature. Equation (3) in Table 1 is the correlation given for turbulent flow parallel to flat plates. Transfer begins at the leading edge. The origin of this correlation is from heat transfer studies.

Kappesser, Greif, and Cornet (1969) found that a constant of 0.0277 for Equation (3) gave a better fit than 0.036 for the evaporation of water from a liquid surface. The Reynolds number range for the experimental measurements was $\simeq 5 \times 10^3$ to 2.88×10^4. The use of a fan in these experiments introduced complicated rotational motion, with vortices starting from the ends of the blades, so that the experimental data for this system are consistent with the results obtained for turbulent flows.

Apparently, Equation (3) is reasonably good for turbulent mass transfer. The use of this equation for a spilled SHICHEM is still invalid because of the sharp edge boundary condition

Kramers and Kreyger (1956) obtained experimental measurements of the rate of solution on rather short surfaces of benzoic acid in water in laminar and turbulent flow. The analysis is treated as the diffusion of a solute from a plane surface into a laminar liquid flow with a constant velocity gradient. The final correlation is shown as Equation (4) in Table 1. This correlation gave a reasonable fit to the experimental data for the experimental R_e range of 1 500 to 7 000. The soluble section was located 330 mm downstream from the water film inlet. A hydrodynamic boundary layer was developed prior to the water encountering the soluble section (5 to 80 mm in length).

The gradient of the water surface of a flowing stream

(that is, sin α) is very nearly equal to the slope of the stream bottom. In the case of open channel flow, it is possible to estimate the gradient $s = \sin \alpha$ from Manning's formula

$$s = 0.0464\, V^2 n^2 / R^{4/3} \qquad (5)$$

Equation (5) is dimensional. Values of n may be obtained from hydraulics handbooks (Davis, 1962).

Harbeck's (1962) studies of evaporation have provided an equation for the mass transfer coefficient for reservoirs having surface areas ranging from 4E3 to nearly 1E8 m^2. Transformed for use in mass transfer to a water phase, the correlation appears as Equation (6) in Table 1. Equation (6) is dimensional. A recent work by Brutsaert (1973) concluded that Harbeck's equation is essentially correct. A note is made that in the transfer equation, the variables should be means taken over periods of a day or less.

Mackay and Matsugu (1973) described the mass and heat transfer processes occurring during the evaporation of liquid hydrocarbons spilled on land and water and developed equations to enable the liquid temperature and evaporation rate to be predicted. Experiments on the evaporation of cumene, water, and gasoline are described and the evaporation mass transfer coefficient correlated with the wind speed, liquid pool size, and the vapor phase Schmidt number. The correlating equation is Equation (7) in Table 1. This equation is dimensional. Comparison of the correlation with flat plate mass transfer correlations shows satisfactory agreement and suggests that turbulent transfer occurs, the rate being enhanced by the liquid surface roughness. Equations (4), (6), and (7) will likely give a reasonable order of magnitude estimates of k_x for flowing natural streams.

As pointed out in the introductory section of this paper, predicting the dissolution rates, dissolution times, and downstream mixing-cup concentrations of spilled SHICHEM are the major goals of this work. The following focuses the available knowledge upon the attainment of these goals.

Consider a quantity of pure SHICHEM of mass M in place upon the bottom of a moving stream of flow rate Q. The chemical displays an interfacial area A and is contained within a zone of contamination A_c (definition: the zone of contamination is the plan area on the bottom of a water environment contained within a single, imaginary, convex line that encircles all the pools, globs, and droplets produced by the spillage, l^2.) The following simple differential equation describes the dissolution rate:

$$\frac{dM_A}{d\theta} = -A(M_A)\, k_x(A)\, (X_{Ao} - X_{Ab}) \qquad (8)$$

where $A(M_A)$, the interfacial area for mass transfer, and $k_x(A)$, the water phase mass transfer coefficient, are some function of interfacial area A.

Some simplifying assumptions can be made as follows: $X_{Ab} = 0$ is valid if the water contains no species A in solution upstream of the spill site. k_x in Equation (8) is shown to be a function of the interfacial area A displayed by the soluble chemical. Equations (2) through (7) indicate that this is so [that is, $L \simeq A^{1/2}$ for Equations (2), (3), (4), and (7)]. However, in the case of a spilled SHICHEM, the pool area (or length) or soluble zone is more nearly analogous to the zone of contamination A. The zone of contamination is formed immediately after the spill and is assumed to remain constant throughout the dissolution process.

The interfacial area for mass transfer is always less than or equal to the zone of contamination. Equation (8) thus further simplifies to

$$\frac{dM_A}{d\theta} = -A(M_A)\, k_x(A_c)\, X_{Ao} \qquad (9)$$

This expression is employed to obtain important water quality predictions associated with the spill. The downstream cup-mixing concentration of species A, $\overline{C}_A$, is the quotient of the mass dissolution rate and the stream volumetric flow rate Q:

$$\overline{C}_A = A(M_A)\, k_x(A_c) X_{Ao}/Q \qquad (10)$$

The spillage lifetime on the bottom θ_A due to the dissolution process is obtained by separating the θ and the M_A variables in Equation (9) and integrating from $\theta = 0$, $M_A = M_{Ai}$ to $\theta = \theta_A$, $M_A = 0$:

$$\theta_A = \frac{1}{k_x(A_c) X_{Ao}} \int_0^{M_{Ai}} \frac{dM_A}{A(M_A)} \qquad (11)$$

The importance of A_c and $A(M_A)$ in predicting $\overline{C}_A$ and θ_A is readily apparent at this point. Some idealized pool and droplet models will further demonstrate this.

DISSOLUTION MODELS

Liquid chemicals at the bottom of a body of water will flow and therefore accumulate in the depressions (that is, potholes). However, some quantities will remain at elevated positions (that is, perched) on the relative flat surfaces above the depressions. Chemicals residing in potholes will assume the shape of the hole. The interfacial area displayed will be a function of the geomteric shape of the hole. Two idealized solid geometric shapes are employed for potholes: constant and variable interface pools. Constant interface pools are those which display a constant chemical-water interfacial area for any chemical depth in the hole. The area is constant and related to pool depth d_{cp}:

$$A_{cp} = M_{cp}/\rho_A d_{cp} \qquad (12)$$

As dissolution proceeds, the volume of liquid remaining in the pool decreases proportional to depth remaining.

Variable interface pools are those which display a variable chemical-water interfacial area dependent upon the remaining depth d_{vp}. A right circular cone of radius d_{vp} and altitude d_{vp} will be employed as a reasonable model of a pool which displays a decreasing area with decreasing mass:

$$A_{vp} = \pi (3M_{vp}/\pi\rho_A)^{2/3} \qquad (13)$$

Liquid residing upon the flat surfaces does so provided interfacial forces result in nonwetting of the bottom material by the liquid chemical. Two idealized solid geometric shapes will be employed for liquid perched on flat bottom surfaces: globs and uniform drops. Globs are shallow, irregularly shaped pools of liquid with flat tops. Height of the glob h_g, is controlled by water-chemical interfacial tension σ and density difference $\Delta\rho$:

$$h_g = \sqrt{2 \cdot \sigma/\Delta\rho \cdot g} \qquad (14)$$

Equation (14) is similar in form and derivation to a relationship for an oil film on water (Langmuir, 1933). The interfacial area of globs is

$$A_g = M_g/\rho_A h_g \qquad (15)$$

As dissolution proceeds, the interfacial tension force causes A_g to decrease proportional to the mass remaining, while h_g remains constant (that is, shrinking glob).

Drops arriving at the bottom of a water body which do not coalesce into pools or globs remain as isolated spheres

TABLE 2. IDEALIZED SHICHEM DISSOLUTION MODELS

Model	Lifetime*	Downstream concentration*
Constant area pools	$T_A = 1$	$C = 1$
Variable area pools	$T_A = 1$	$C = 3(1-T)^2, T \leq 1$
Shrinking globs	$T_A\dagger = 3$	$C = \exp(-T)$
Uniform drops	$T_A = \frac{1}{2}$	$C = 6(1-2T)^2$ $T \leq \frac{1}{2}$

† 95% in solution.

* Definitions: $T \equiv \theta/\phi_m$, $C_A \equiv \overline{C_A}/\gamma_m$, $\phi_m \equiv \rho_A L/k_x X_{Ao}$, $\gamma_m \equiv M_{Ai}/\phi_m Q$.

positioned upon the bottom. The bottom will undoubtedly be spattered with drops of various diameters. An equation is available for estimating the maximum stable diameter d of a drop falling through water (Hu and Kintner, 1955):

$$d = 0.12\sqrt{\sigma/\Delta\rho} \tag{16}$$

The interfacial area of uniform drops is

$$A_d = \pi(6M_d/\pi\rho_A)^{2/3} \tag{17}$$

The downstream cup-mixing concentration [Equation (10)] and spillage lifetime [Equation (11)] can be completely specified based upon the above four models. In all cases, as dissolution proceeds, the mass of SHICHEM will decrease. However, depending upon the model chosen, concentration and lifetime will vary considerably. For this reason each model must be developed separately.

Constant Interface Pool Model

In this model dissolution occurs from the top of the pool and peels away successive layers (so to speak) of area A_{cp}. Substituting Equation (12) into Equation (11), we get the pool lifetime:

$$\theta_{cp} = \rho_A d_{cp}/k_x X_{Ao} \tag{18}$$

Equation (10) also combined with Equation (12) yields the downstream concentration of SHICHEM resulting from pools of constant interface:

$$\overline{C_{cp}} = k_x M_{cp} X_{Ao}/\rho_A d_{cp} Q \tag{19}$$

The concentration is constant and persists for θ_{cp} at which time the pothole contains no SHICHEM.

Variable Interface Pool Model

In this model dissolution occurs from the top also. However, interfacial area decreases with mass remaining. Substituting Equation (13) into Equation (11), we get the pool lifetime

$$\theta_{vp} = \rho_A d_{vp}/k_x X_{Ao} \tag{20}$$

plus a relationship between mass remaining and time. Putting this mass time relation and Equation (13) into Equation (10), we get the downstream concentration of SHICHEM resulting from pools of variable interface:

$$\overline{C_{vp}} = \frac{3k_x M_{vp} X_{Ao}}{\rho_A d_{vp} Q}\left(1 - \frac{k_x X_{Ao}\theta}{\rho_A d_{vp}}\right)^2 \tag{21}$$

where θ is time (t) such that $\theta \leq \theta_{vp}$. The concentration is maximum at the time of spill ($\theta = 0$) and decreases with the square of time until the pothole contains no SHICHEM.

Shrinking Glob Model

It is assumed that globs are somewhat large so that the perimeter interfacial area is small compared to the top interfacial area. This assumption is invalid as glob diameter approaches h_g. At this point, the glob becomes a drop. Dissolution is assumed to occur from the top only so that area

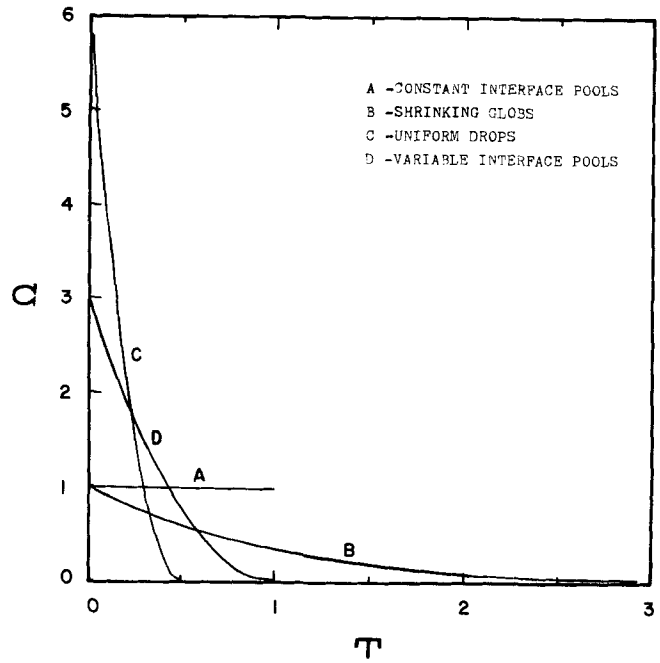

Fig. 2. Idealized SHICHEM dissolution models.

is directly proportional to mass remaining. Substituting Equation (15) into Equation (11), we get a mass time relationship from which the lifetime can be estimated:

$$\theta_g = \frac{\rho_A h_g}{k_x X_{Ao}} \ln(1/f) \tag{22}$$

where f is some small fraction of SHICHEM remaining, but, for all practical purposes, the dissolution process is completed. A reasonable f is 0.05 (that is, 5% undissolved) and $\ln(1/f) \simeq 3$. The downstream concentration of SHICHEM resulting from shrinking globs is

$$\overline{C_g} = \frac{k_x M_g X_{Ao}}{\rho_A h_g Q}\exp\left(\frac{-k_x X_{Ao}\theta}{\rho_A h_g}\right) \tag{23}$$

Uniform Drop Model

Equation (16) provides a reasonable estimate of the maximum diameter of SHICHEM drops upon the bottom. Dissolution is assumed to proceed such that the drops remain spherical with decreasing diameter. Equation (17) substituted into Equation (11 yields a mass time relationship from which the lifetime can be obtained:

$$\theta_d = \rho_A d/2k_x X_{Ao} \tag{24}$$

The downstream concentration of SHICHEM from drops is obtained from Equation (10):

$$\overline{C_d} = \frac{6k_x M_d X_{Ao}}{\rho_A d Q}\left(1 - \frac{2k_x X_{Ao}\theta}{\rho_A d}\right)^2 \tag{25}$$

Equations (18) through (25) represent the details of the dissolution models. Reduction to dimensionless variables summarizes the essence of the models. Let $\phi_m \equiv \rho_A L/k_x X_{Ao}$ (where L is d_{cp}, d_{vp}, h_g, or d) be a mass transfer time constant and $\gamma_m \equiv M/\phi_m Q$ (where M is M_{cp}, M_{vp}, M_g, or M_d) be a characteristic spill concentration. Define a dimensionless time $T \equiv \theta/\phi_m$ and a dimensionless concentration $C \equiv \overline{C}/\gamma_m$. Table 2 contains the summary of the dimensionless model equations. Figure 2 is a graphical representation.

The total mixing-cup concentration-time history of the spilled chemical at mile 0.0 is the sum of the contribution from each source:

$$\overline{C} = C_{cp} + C_{vp} + C_g + C_d \tag{26}$$

Substituting for the appropriate expressions from Equations (19), (21), (23), and (25), we get the concentration-time history in the flowing stream:

$$\overline{C} = \frac{k_x X_{Ao}}{\rho_A Q}\left\{\frac{M_{cp}}{d_{cp}} + \frac{3M_{vp}}{d_{vp}}\left(1 - \frac{k_x X_{Ao}\theta}{\rho_A d_{vp}}\right)^2 + \frac{M_g}{h_g}\exp\left(\frac{-k_x X_{Ao}\theta}{\rho_A h_g}\right) + \frac{6M_d}{d}\left(1 - \frac{2k_x X_{Ao}\theta}{\rho_A d}\right)^2\right\} \quad (27)$$

Both squared terms on the right-hand side must be positive or zero before squared; otherwise they are not included. Also

$$M = M_{cp} + M_{vp} + M_g + M_d \quad (28)$$

must be satisfied.

Equation (27) is useful for estimating instream concentration of the spill of SHICHEM. Many terms in this equation can be obtained a priori. However, there remains five unknown pieces of information. Stream flow (Q) and the quantity spilled (M) can be obtained from the spill site, actual or projected. The mass transfer coefficient (k_x), glob height (h_g), and drop diameter (d) can be estimated from equations presented in this paper. Solubility (X_{Ao}) and density (ρ_A) are available in handbooks. The remaining six variables (M_{cp}, M_{vp}, M_g, M_d, d_{cp}, and d_{vp}) can be reduced to five by employing Equation (28). The five remaining variables must be specified from a special knowledge of the stream bottom at the spill site to yield a realistic concentration-time prediction. In the absence of stream bottom information, the individual models can yield reasonable estimates of concentration and lifetime due to a projected spill.

Neely, Blau, and Turner (1976) developed a mathematical model that has a predictive capability. Chloroform spill data (Daigre, 1976) was employed. The river was visualized as a series of continuous stirred-flow compartments. Material balances for the flow of contaminant through the compartments results in differential equations. As many as 121 simultaneous differential equations representing 121 compartments were successfully integrated. Evaporation at the air-water interface and dissolution at the bottom are incorporated into the model. Four parameters were adjusted until the concentration-time profiles were generated corresponding to the data collected at mile 16.3 and mile 121, respectively. The close agreement between the calculated and observed values lends credence to the model representation.

The model developed in this paper and the model of Neely, Blau, and Turner are complementary for the most part. The model presented here is concerned with the specific spill phenomena and the dissolution mechanism occurring on the bottom at the spill site and not concerned with downstream prediction. The Neely, Blau, Turner model is only cursorily concerned with the dissolution mechanism but is comprehensive with respect to downstream prediction.

CHLOROFORM SPILL

In 1973 a major spill involving chloroform occurred on the Mississippi River at Baton Rouge, Louisiana. The documentation and surveillance of this spill by the Louisiana Division of the Dow Chemical Company (Daigre, 1976) provides a unique field experiment upon which to evaluate predictive models for the dissolution of high density chemicals in flowing environments.

On August 19, 1973, a barge carrying three tanks of chloroform for midwestern terminals was damaged on the Mississippi River at Baton Rouge, Louisiana, during make-up of an upriver tow. While being repaired, the barge collapsed in the middle and sank at its moorings as preparations to unload were getting underway. The contents of two 265 m^3 tanks were lost. The first tank ruptured at 2:40 p.m., releasing its entire contents in a short period of time. The second tank sprang a leak at 10:00 p.m. the same day and released its contents over a 45 min period. An estimated total of 7.7E5 kg of chloroform was lost to the river.

The spill occurred at river mile 226 which is the distance from the Gulf of Mexico outlet. The river was at low stage at Baton Rouge flowing at 7590 m^3/s. The water temperature was 28°C.

TABLE 3. CHLOROFORM SPILL IN MISSISSIPPI RIVER (DAIGRE, 1976)

Date	Hr*	$CHCl_3$ in river** mg/m^3	Date	Hr*	$CHCl_3$ in river** mg/m^3
8/19	2330	80		2000	33
8/20	0030	220		2400	28
	0130	264	8/23	0400	25
	0230	352		0930	22
	0245	264		1330	31
	0330†	365		1800	39
	0430	326		2400	28
	0630	233	8/84	0400	25
	0730	202		0900	31
	0830	162		1330	31
	0930	121		1600	24
	1030	121	8/25	0400	24
	1130	121		0800	21
	1230	121		2350	26
	1330	101	8/26	0900	21
	1530	81		1600	20
	1730	59		2400	22
	1930	81	8/27	1620	21
	2330	61	8/28	0800	15
8/21	0130	70	8/29	0800	6
	0230	70	8/30	0800	13
	0730	81	8/31	0800	12
	1430	70	9/4	0800	4
	1830	64	9/5	0800	3
8/22	0600	53	9/6	0800	7
	1600	42	9/7	0800	3

* Sample time at mile 16.3
† Chose 8/20 @ 0330 as $\theta = 0$.
** Concentration at mile 16.3 multiplied by 1.1.

TABLE 4

A. Mississippi River characteristics at spill site

Volumetric flow	7 590 m^3/s	Temperature	28°C
Velocity	56.3 cm/s	Spill site-Baton Rouge, La.,	0.0 mi
Width	1 800 m	Sample site-Plaquemine, La.,	16.3 mi
Depth	16.5 m	Water travel time	10 hr

B. Chloroform properties and calculated spill parameters

1. Chloroform properties at 20°C:
   - Solubility: 0.82 g/100 g H_2O (X_{Ao} = 1.24E-3)
   - Density: 1.489 g/cm^3
   - Interfacial tension: 0.0328N/m
2. Mass of spill:
   - Lost from barges: 770 000 kg
   - Accounted in river: 317 000 kg
3. Calculated parameters:
   - Glob height, Equation (14): h_g = 0.366 cm
   - Drop diameter, Equation (16): d = 0.976 cm
   - Mass transfer coefficient, Equations (4), (6), (7): k_x = 0.60 g·mole/s·m^2

The Dow Chemical Company, Louisiana Division, is located 16.3 mi below the point of the spill at river mile 209.9. Mississippi River water is taken into the division at a rate of 32 m^3/s. Beginning at 5:30 p.m., August 19, samples of intake water were taken every hour and analyzed for chloroform. The normal chloroform concentration in the Mississippi River at this river stage is <5 mg/m^3. An increase above this level was noted at 10:30 p.m. with a maximum concentration reaching 330 mg/m^3 at 3:30 a.m. on August 20. Samples were taken at regular intervals for the next week and at irregular intervals up to 3 wk.

Water samples were analyzed using vapor phase partitioning and gas chromatographic analysis. The sensitivity of the method for chloroform in water was 5 mg/m^3 using flame ionization. Standards were made by adding a known weight of chloroform to water. After it was mixed, the water was partitioned with nitrogen and a 2 cm^3 sample of gas injected into the chromatograph. All concentrations were based on peak height.

Approximately 242 000 kg of chloroform was accounted for at the 16.3 mi location, and 177 000 kg had passed New Orleans 8 days after the spill occurred. This indicates that 27% of the chloroform was lost by desorption to the air or adsorption onto the river silt or mud. An evaporation constant for chloroform of 2.16E-3 cm/s was used by the present author to correct the 16.3 mi concentration data back to the spill site (that is, mile 0.0). Table 3 contains the concentration time data which accounts for 317 000 kg. Table 4A contains pertitnent river data near the spill site and the sample site.

The flow time from the spill site to mile 16.3 is approximately 10 hr. The lapse time from the start of the spill (August 19, 2:40 p.m.) to the arrival of high levels of chloroform in river water (August 19, 10:30 p.m.) was 7 hr, 50 min. Leakage of chloroform from the barge ceased at approximately 11:00 p.m. on August 19. A 10 hr flow time to mile 16.3 results in an estimated time of arrival of 9:00 a.m. August 20. If we allow for some backmixing in the river, chloroform concentration should have returned to background levels (that is, ~ 5 mg/m^3) on August 21 or soon thereafter. However, significant levels of chloroform were present in the river water for 12 days (August 31) following the spill, indicating that quantities of the chemical were upon the bottom and dissolution was occurring.

DISSOLUTION MODEL PREDICTIONS

The spill data presented in Table 3 represent the approximate concentration-time profile that would have resulted at the spill site. The dissolution model equation [Equation (27)] represents the concentration-time profile at the point immediately downstream of the spill of a quantity M by proper adjustment of five parameters. The five adjustable parameters are M_{cp}-mass contained in constant area pools, M_{vp}-mass in variable area pools, M_d-mass in uniform drops, d_{cp}-depth of constant area pools, and d_{vp}-depth of variable area pools.

As a demonstration of the predictive capability of the dissolution model from an a priori approach, a reasonable distribution of mass and reasonable dimensions were as-

TABLE 5. CHLOROFORM SPILL PREDICTED MAXIMUM RIVER CONCENTRATIONS AND MINIMUM LIFETIMES

Bottom forms	Concentration Equation	Concentration mg/m³†	Lifetime Equation	Lifetime Days
Constant interface pools*	19	155-64	18	1.9
Variable interface pools*	21	465-192	20	1.9
Shrinking globs	23	414-170	22	2.1
Uniform drops	25	931-383	24	.95
Total	26	1 965-809	—	—

* Pool depths assumed to be 0.366 cm.
† Maximum is based on 770 000 kg and minimum is based on 317 000 kg.

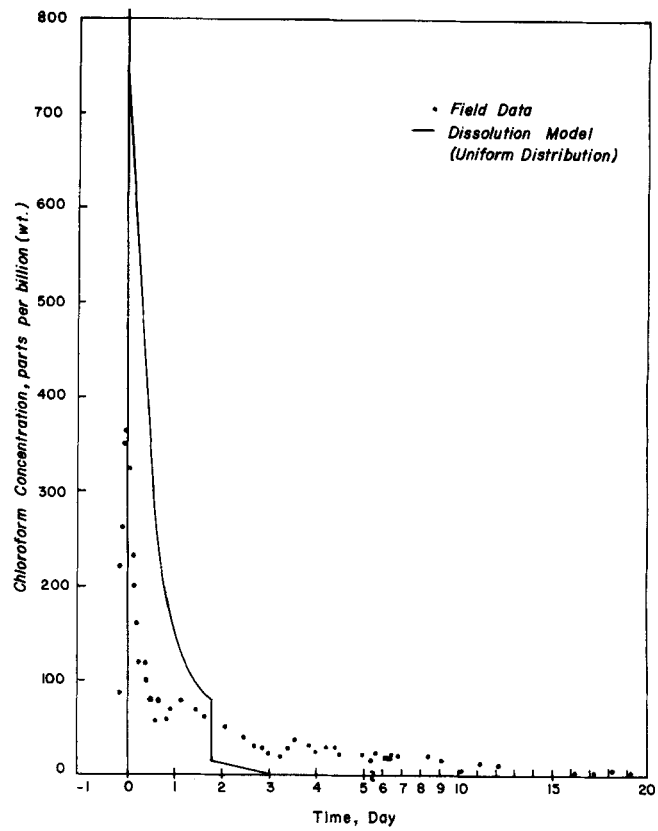

Fig. 3. Chloroform spill in Mississippi river.

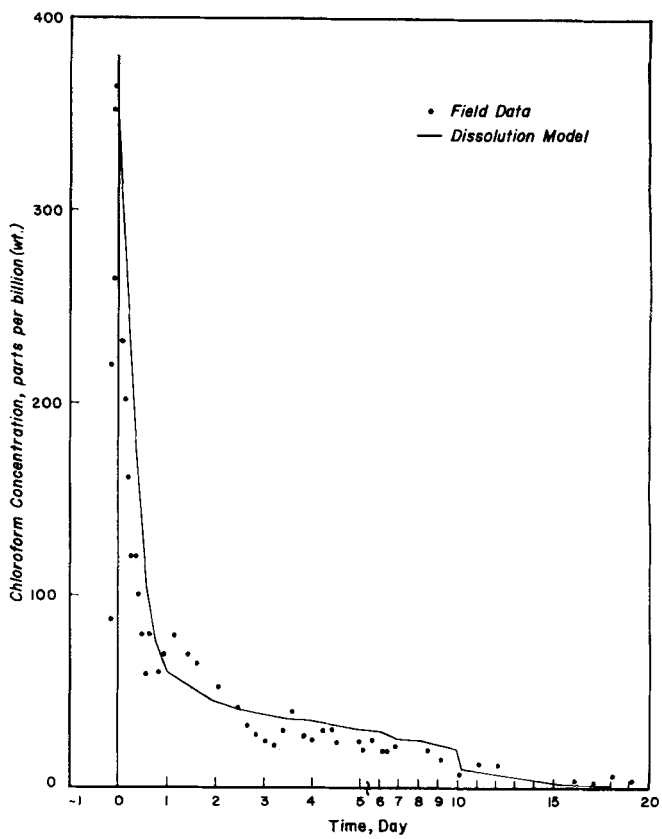

Fig. 4. Chloroform spill in Mississippi river.

sumed to construct a preliminary concentration-time profile of the chloroform spill. The four bottom forms of deposited chloroform mass were assumed to be uniformly distributed. For the case of a 7.7E5 kg spill, 1.93E5 kg were contained in each form; for the case of a 3.17E5 kg spill, 7.94E4 kg were contained in each form. Equation (14) was employed to estimate drop diameter (0.98 cm.). Six correlations were used to estimate the mass transfer coefficient k_x, see Table 1. An average value of 0.6 g-mole/s · m² based on three correlations representing field conditions, as opposed to idealized laboratory conditions, was used. Table 4B summarizes the data and other calculations employed for the a priori prediction. Maximum river water concentrations and expected lifetimes are presented in Table 5. Figure 3 contains the predicted concentration-time profile and also contains the field observations.

The strength of a predictive model is evaluated partially in light of its capability of reproducing the observed field data. Little credence is given to a model in which adjustment of the unknown parameters results in failure to mimic the major features of the field observations. Figure 4 represents a simulation of the data. Numerical values of the adjustable parameters used to obtain this simulation were $M_{cp} = 65\,530$ kg, $M_{vp} = 165\,200$ kg, $M_d = 54\,150$ kg, $d_{cp} = 5.16$ cm, and $d_{vp} = 10.3$ cm. Six adjustments, by hand calculator, were attempted to yield the final parameters. No attempt was made to obtain unique values of the unknown parameters in a least-squares sense.

DISCUSSION

The total mass of chloroform lost to the river was approximately 7.7E5 kg, but only 2.42E5 kg was accounted for at mile 16.4 downstream from the spill site. Desorption coefficients from evaporation studies of five low molecular weight chlorinated hydrocarbons including chloroform (Dilling et al., 1975) made it possible to correct the 16.3 mi field observations for the loss of chloroform through the water-air interface. A total of 3.17E5 kg can be accounted for considering evaporation losses. Dilling also studied the adsorption of chlorinated hydrocarbon from dilute aqueous solutions and reported significant uptake results on bentonite clay (10 to 22%), dolomitic limestone (50 to 90%), peat moss (40%) but no uptake by Ottawa silica sand. It appears that the river bottom material is a likely sink to entrap significant quantities of chloroform.

The dissolution model is designed to predict concentration-time profiles at the point of spill. The uniform mass distribution model results are presented in Table 5 and Figure 3. Table 5 contains maximum instream concentrations of chloroform based upon the 770 000 kg known loss and the 317 000 kg accounted for. The table also contains estimates of the spill dissolution time. These time computations are minimums because pool depths are underestimated by Equation (14). The divergence of the uniform mass distribution simulation from the field data shown in Figure 3 results in part from the underestimated pool depths also. Divergence is also attributed to a lack of information on the distribution of material in the potholes upon the stream bottom.

Figure 4 is an adequate simulation of the field data. The adjustment of the five unknown parameters to obtain this simulation reveals something of the geometric makeup of the river bottom at the spill site. The mass of chloroform deposited as globs and drops totaled 86 750 kg. This material resides at perched positions upon the bottom in thin layers of approximately 4/10 cm thick and spherical drops of up to approximately 1 cm in diameter. These small geometric forms have high surface area-to-volume ratios and result in the high concentrations observed between time 0 and 2 days. The mass of chloroform deposited in potholes (that is, pools) totaled 230 730 kg. This material resides in depressions in the bottom, resulting in pools of chloroform 5 to 10 cm deep. These pools display relatively low exposed interfacial area per unit volume, resulting in lower instream concentrations and longer dissolution times as observed between day 2 and day 10. The abrupt drop in the dissolution model concentration at day 10 is the result of the depletion of chloroform from the constant area pools. The decreasing concentration tail between day 10 and 15 is attributed to the small quantities of chloroform in the bottom of potholes (that is, tip of the cone).

CONCLUSIONS

The interfacial area production phenomenon and the subsequent dissolution of a liquid chemical ($\rho > 1$) spilled in a natural flowing stream is complex, and attempts at quantitative description suffer from the lack of controlled laboratory experimental data to affect a comparison. Realistic field experiments are costly and possibly polluting in their execution. On-site monitoring of accidental spills does provide field data against which to compare quantitative dissolution models. This paper presents an attempt at quantitative description for the important class of chemical spill hazards. The following items are concluded:

1. Aspects of the engineering science of liquid-liquid extraction provide a plausible basis upon which to construct liquid chemical spill mechanisms which result in a zone of contamination upon the stream bottom.
2. Simple geometric shapes which include drops, globs, and pools are sufficient to describe the forms assumed by the bottom residing liquid. The exact nature of these bottom forms, which includes the distribution of mass of liquid in the various shapes and the depth of chemical, emerge as important parameters.
3. Reasonably accurate a priori predictions of lifetime and concentration can be made based upon published mass transfer rates, a uniform distribution of bottom forms, spill site information, and basic physical and chemical properties of the spilled liquid.

NOTATION

A = interfacial area, l^2
C = dimensionless concentration, $\overline{C}_A/\gamma_m$
$\overline{C}$ = instream cup-mixing concentrations, m/l^3
c, c_m = bulk concentration, mass and molar, m/l^3 or mole/l^3
$\mathcal{D}_{AB}$ = molecular diffusivity of A in B, l^2/t
d = diameter of droplet, l
f = fraction, $0 \leq f \leq 1.0$
g, g_x = gravitational acceleration and vertical component ($g_x = g \sin\alpha$), l/t^2
h = pool depth, l
k_x = liquid phase mass transfer coefficient, mole/$l^2 \cdot t$
L = length of pool, l
M = mass of spill, m
M_{Ai} = initial mass quantity of species A spilled, m
n = coefficient of roughness
Q = stream volumetric flow rate, l^3/t
R = hydraulic radius of stream, l
Re = Reynolds number, $L\overline{V}\rho/\mu$
Sc = Schmidt number, ν/D_{AB}
s = stream channel slope, l/l
T = dimensionless time, θ/ϕ_m
V = volume of spill, l^3
V_x, V_w, $\overline{V}$ = velocity far removed from interface, wind and average, l/t
W_A = interphase mass flux rate of component A, mole/t

X_{Ao}, X_{Ab} = mole fraction of component A in water, at interface, bulk

Greek Letters

α = angle of stream bottom from horizontal, deg
γ_m = a defined concentration, $M_A/\phi_m Q$, m/l^3
Γ_v = volumetric flow rate per unit channel bottom width, l$^3/t \cdot$ l
π = 3.1416...
ρ_A = density of material A, m/l^3
σ = interfacial tension, F/l
θ, θ_A = time, lifetime of spillage, t
ν = kinematic viscosity, μ/ρ, l$^2/t$
μ = viscosity, m/l $\cdot$ t
ϕ_m = defined time, $\rho_A L/k_x X_{Ao}$, t

Subscripts

A = chemical component A
c_p = constant area pool
d = drop or droplet
g = glob
v_p = variable area pool
w = water
x = vertical component

LITERATURE CITED

Bird, R. B., W. E. Stewart, and E. N. Lightfoot, *Transport Phenomena*, p. 640, Wiley, New York (1960).

Brutsaert, W., Heat and Water Vapor Exchange Between Water Surface and Atmosphere, EPA-R2-73-259, Office of Res. and Monitoring," U.S.E.P.A., Washington, D. C. (1973).

Chen, E. C., J. C. K. Overall, and C. R. Phillips, "Spreading of Crude Oil on an Ice Surface," *Can. J. Chem. Eng.*, **52**, 71 (1971).

Dahm, B. B., R. J. Pilie, and J. P. Lafornara, "Technology for Managing Spills on Land and Water," *Env. Sci. Technol.*, 8, 1076 (1974).

Daigre, G. W., Dow Chemical Company provided data on the chloroform spill and water sample analysis results, private communication (Apr. 1, 1976).

Davis, C. V., ed., *Handbook of Applied Hydrology*, p. 1204 McGraw-Hill, New York (1962).

Dilling, W. L., N. B. Tefertiller, and G. J. Kallos, "Evaporation Rates and Reactivities of Methylene Chloride, Chloroform, 1,1,1-Trichloroethane, Trichloroethylene, Tetrachloroethylene, and Other Chlorinated Compounds in Dilute Aqueous Solutions," *Env. Sci. Technol.*, 9, No. 9, 833 (Sept. 1975).

Dzubur, I., and H. Sawistowski, "Effect of Direction of Mass Transfer on Breakup of Liquid Jets," *Proc. Intern. Solvent Extraction Conf.*, 1, 379 (1974).

Edge, R. M., and I. E. Kalafatoglu," The Breakup of Chlorobenzene Drops Falling Freely Through Water," *ibid.* (1974).

Fay, J. A., "Physical Processes in the Spread of Oil on a Water Surface," *Proc. Joint Conf. on Prevention and Control of Oil Spills*, p. 463, API, Washington, D. C. (1971)

Harbeck, G. E., Jr., "A Practical Field Technique for Measuring Reservoir Evaporation Utilizing Mass-Transfer Theory," *Geol. Survey Prof. Paper 272-E* U.S. Govt. Printing Office, Washington, D. C. (1962).

Hayworth, C. B., and R. E. Treybal, "Drop Formation in Two-Liquid-Phase Systems," *Ind. Eng. Chem.*, **42**, 1174 (1950).

Hu, S., and R. C. Kintner, "The Fall of Single Liquid Drops Through Water," *AIChE J.*, **1**, 42 (1955).

Jones, K. R., and D. Verser, "Dispersion and Dissolution of Soluble, High Density Chemicals Spilled in Aqueous Environments," Univ. Ark., Fayetteville (May, 1974).

Kappeser, R., R. Greif, and I. Cornet, "Evaporation Retardation by Monolayers," *Science*, **166**, 403 (1969).

Kramers, H., and P. J. Kreyger, "Mass Transfer between a Flat Surface and a Falling Liquid Film," *Chem. Eng. Sci.*, **6**, 42 (1956).

Langmuir, I., "Oil Lenses on Water and the Nature of Monomolecular Expanded Films," *J. Chem. Physics*, 1, 756 (1933).

Mackay, D., and R. S. Matsugu," Evaporation Rates of Liquid Hydrocarbon Spills on Land and Water," *Can. J. Chem. Eng.*, **51**, 434 (1973).

Meister, B. J., and G. F. Scheele, "Prediction of Jet Length in Immiscible Liquid Systems," *AIChE J.*, **15**, 689 (1969).

———, "Drop Formation from Cylindrical Jets in Immiscible Liquid Systems," *ibid.* (1969).

Neely, W. B., G. E. Blau, and A. Turner, Jr., "Mathematical Model Predicts Concentration-Time Profiles Resulting from Chemical Spill in a River," *Env. Sci. Technol*, **10**, 72 (Jan., 1976).

O'Brien, J. A., "Oil Spreading on Water from a Stationary Leaking Source," *Chem. Eng.*, CE 407 (Dec., 1970).

Pilie, R. S., et al., "Methods to Treat, Control and Monitor Spilled Hazardous Materials," pp. 127-136, U.S.E.P.A., Cincinnati, Ohio, *EPA-670/2-75-042* (1975).

Schooley, A. H., "Evaporation in the Laboratory and at Sea," *J. Mar. Res.*, **27**, 335 (1969).

Siemer, W., and J. F. Kaufman, "Tropfenbilding in Flusskgkeiten an Dusen bei hohen Durchcatz," *Chemie-Eng. Tech.*, **29**, p. 63, 32 (1957).

Treybal, R. E., *Mass-Transfer Operations*, p. 63, McGraw-Hill, New York (1968).

Vijayan, S., and A. B. Ponter, "Coalescence in a Laboratory Continuous Mixer-Settler Unit: Contributions of Drop/Drop and Drop/Interface Coalescence Rates on the Separation Process," *Proc. Int. Solvent Extraction Conf.*, 1, 591 (1974).

Manuscript received June 14, 1976; revision received April 13, and accepted May 12, 1977.

Magnetothermal Convection of Oxygen Gas In Nonuniform Magnetic Fields

Natural convection heat transfer through oxygen gas may be significantly altered by the application of a nonuniform magnetic field. An additive contribution to the point velocity arises from the temperature dependence of the magnetic body force on the fluid. Theoretical predictions are in close agreements with experimental results.

DONALD C. CLARK
and
WALLACE I. HONEYWELL

Chemical Engineering Department
University of Houston
Houston, Texas 77004

SCOPE

In 1972, Honeywell et al. (1972) reported an unexpectedly large increase (20 to 50%) in the apparent thermal conductivity of oxygen gas at 77°K when a steady, uniform, magnetic field was applied to the gas under the influence of a small temperature gradient. These experimental results were anomalous both in the magnitude and sign of the effect. Previous experimental results and the kinetic theory of the Senftleben-Beenakker thermal conductivity effect (Bennakker and McCourt, 1970) sug-

Correspondence concerning this paper should be addressed to Wallace I. Honeywell. Donald C. Clark is with The Rohm and Haas Company, Philadelphia, Pennsylvania, 19132.